A SHEAR-STRENGTH-DERIVED LITHOLOGICAL WEAKNESS INDEX FOR GIS-BASED LANDSLIDE SUSCEPTIBILITY MODELLING IN MOUNTAINOUS ROAD CORRIDORS OF NORTHERN VIETNAM

Thanh Long NGUYEN [1], ***Thi Ngoc Ha TRAN*** [1], ***Quoc Lap KIEU*** [1*]
& Dieu Trinh NGUYEN [2]

DOI: 10.21163/GT_2026.212.10

ABSTRACT
Lithology is commonly incorporated into landslide susceptibility models as a categorical map variable, although this representation may not adequately express the mechanical behaviour of slope-forming materials. To improve the physical interpretability of lithological information without substantially changing the conventional GIS-based modelling workflow, this study introduces a shear-strength-informed lithological standardization approach for landslide susceptibility assessment in a mountainous road-corridor environment. Conventional lithological groups were converted into a Lithological Weakness Index (LWI) derived from laboratory-measured cohesion and internal friction angle from 58 samples, and the index was integrated into a Random Forest modelling framework. The approach was tested along National Road QL279 in Lao Cai Province, northern Vietnam, using topographic, environmental, rainfall, geological, hydrological, infrastructural and landslide-inventory data. The RF-LWI model achieved an AUC-ROC of 0.936, accuracy of 0.865 and F1-score of 0.847 on the independent testing dataset, with a mean cross-validated AUC-ROC of 0.943. High and very high susceptibility classes covered 52.71% of the study area. Compared with the model using conventional reclassified lithology, the LWI-based model produced only a modest improvement in predictive performance, but it provided a more mechanically meaningful and interpretable representation of lithological control. The results indicate that shear-strength-derived lithological standardization is useful mainly as a refinement of the geological predictor rather than as a source of large accuracy gains. This approach may support more transparent GIS-based landslide susceptibility modelling in mountainous road corridors where lithological heterogeneity and road-related slope disturbance interact.

Keywords: *Landslide susceptibility; Lithological Weakness Index; Shear strength; Random Forest; GIS-based modelling.*

1. INTRODUCTION

Landslides are common geomorphic hazards in mountainous regions, where slope instability is controlled by interactions among relief, lithology, rainfall, drainage, vegetation cover and human disturbance. Their consequences are particularly significant along mountain road corridors, because slope failures may disrupt transport, damage infrastructure, increase maintenance costs and reduce access to local communities. In such settings, landslide susceptibility mapping provides a spatial basis for identifying terrain sectors with different propensities to failure and for supporting road maintenance, land-use planning and disaster-risk reduction (Guzzetti et al., 1999; Fell et al., 2008; Van Westen et al., 2008; Reichenbach et al., 2018).

[1] *Thai Nguyen University of Sciences, Thai Nguyen Province, Vietnam, longgeoj@gmail.com (TLN), hattn@tnus.edu.vn (TNHT), lapkq@tnus.edu.vn (QLK)*
[2] *Vietnam Academy of Science and Technology, Hanoi City, Vietnam, nguyendieutrinh70@gmail.com (DTN)*
[*] *Corresponding author: lapkq@tnus.edu.vn*

The development of remote sensing, GIS and spatial modelling has improved the representation of landslide-conditioning factors at regional and corridor scales. Digital elevation models, satellite imagery, land-cover datasets, gridded rainfall products and geological maps are frequently combined to describe topographic, hydrological, environmental, lithological and anthropogenic controls on slope instability (Drusch et al., 2012; Funk et al., 2015; Brown et al., 2022). Recent studies have applied GIS, remote sensing, multi-criteria evaluation, machine learning and spatial analysis to landslide susceptibility, landslide vulnerability, flash-flood hazard and disaster-risk mapping in diverse mountain environments (Zhanabayev et al., 2024; Dahmani et al., 2025; Edial et al., 2025). These studies demonstrate the importance of spatially explicit and technically reproducible approaches for natural-hazard assessment.

Among data-driven approaches, machine-learning algorithms have been widely used in landslide susceptibility modelling because they can represent nonlinear relationships between landslide occurrence and multiple conditioning variables. Random Forest is among the most frequently applied algorithms, as it can handle mixed data types, reduce sensitivity to noisy predictors and provide variable-importance measures that support geomorphological interpretation (Breiman, 2001; Catani et al., 2013; Chen et al., 2018; Merghadi et al., 2020; Ado et al., 2022). However, the reliability of machine-learning susceptibility models depends not only on the algorithm, but also on the quality of the landslide inventory, the definition of non-landslide samples, the spatial resolution and scale of input factors, the treatment of class imbalance and the validation strategy (Conoscenti et al., 2016; Steger et al., 2017; Tanyu et al., 2021; Gu et al., 2023; Gu et al., 2024; Kanwar et al., 2025). These issues are especially relevant in road-corridor studies, where landslide and non-landslide samples may occur within narrow terrain belts affected by slope cutting, drainage modification and short-distance changes in lithology.

One remaining issue concerns how lithological information is represented in susceptibility models. Lithology is commonly used as a categorical predictor derived from geological maps. Although this representation is practical, it does not always express the mechanical behaviour of slope-forming materials. Geological units with different names may have comparable strength properties after weathering, whereas units assigned to the same lithological class may differ in cohesion, internal friction angle, discontinuity conditions, weathering grade and permeability. As a result, the direct use of nominal lithological classes can limit the physical interpretation of geological control in statistical or machine-learning susceptibility models (Bunn et al., 2020; Segoni et al., 2020; Yu et al., 2021).

A more interpretable lithological predictor should be linked, where data allow, to material properties that influence slope resistance. Cohesion and internal friction angle are particularly relevant because they are directly associated with shear strength. Cohesion reflects the bonding or cementation component of shear resistance, whereas the internal friction angle represents frictional resistance along potential failure surfaces. Previous studies have emphasized that geological and rock–soil factors can improve landslide susceptibility assessment when they are parameterized in relation to material behaviour rather than used only as map-based categories (Bunn et al., 2020; Segoni et al., 2020; Yu et al., 2021).

Nevertheless, laboratory-derived shear-strength parameters are still rarely incorporated into GIS-based susceptibility models as a standardized lithological variable. This gap is important because a shear-strength-informed lithological variable may improve the interpretability of the geological predictor, even if the resulting gain in predictive accuracy is modest. This issue is particularly relevant for mountainous road corridors, where lithological heterogeneity, slope cutting, modified drainage and rainfall-induced processes interact within narrow spatial zones.

Northern Vietnam provides a suitable setting for examining this problem. The mountainous part of the country is characterized by steep relief, deeply dissected valleys, monsoonal rainfall, complex geological conditions and expanding transport infrastructure. Previous studies have shown the usefulness of GIS, remote sensing and spatial modelling for landslide, flash-flood and disaster-risk assessment in this region (Bui et al., 2011; Kieu and Tran, 2021; Kieu and Ngo, 2022; Do et al., 2025; Kieu and Tran, 2025). However, limited attention has been given to whether conventional lithological

classes can be refined by using measured shear-strength properties before their integration into machine-learning susceptibility models. In corridor-scale studies, this refinement should be interpreted as a practical group-level standardization of lithological weakness rather than as a complete geotechnical characterization of each geological unit.

This study addresses this issue by proposing a shear-strength-informed lithological standardization approach for GIS-based landslide susceptibility modelling in a mountainous road corridor. The study converts reclassified lithological groups into a Lithological Weakness Index derived from laboratory-measured cohesion and internal friction angle, and then tests whether this standardized lithological variable improves Random Forest susceptibility modelling compared with conventional lithological representation. The proposed index is intended as a transparent proxy for relative lithological weakness and as a refinement of the geological predictor, not as a replacement for field-based engineering-geological investigation. The approach is evaluated along a mountainous road corridor in northern Vietnam using a multi-source spatial database, a landslide inventory, geomechanical samples and repeated model validation. The specific objectives are: (1) to prepare a GIS-based database of landslide-conditioning factors for a mountainous road corridor; (2) to derive a shear-strength-based Lithological Weakness Index for reclassified lithological groups; (3) to develop and validate a Random Forest landslide susceptibility model; and (4) to compare the performance of conventional lithology and shear-strength-standardized lithology. By linking lithological representation to measured material strength, the study aims to improve the physical interpretability of the geological predictor while retaining a transferable GIS-based workflow for landslide susceptibility assessment in mountainous transport corridors.

2. STUDY AREA

The study area is located along National Road QL279 in Lao Cai Province, northern Vietnam (**Fig. 1**), within the mountainous upper Red River region.

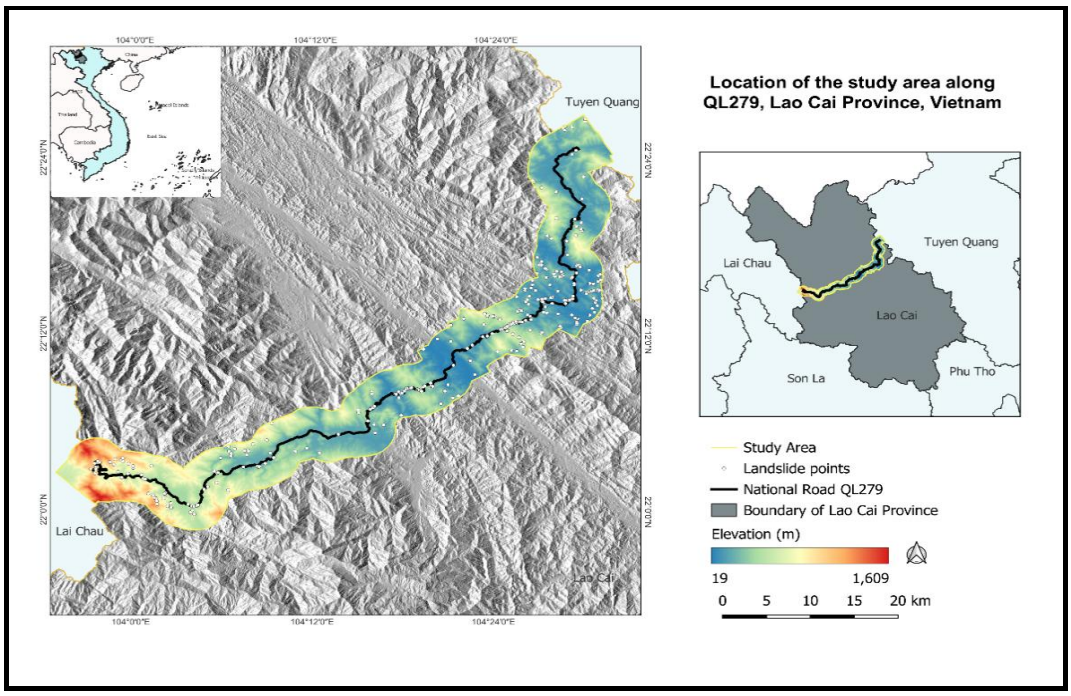

Fig. 1. Location of the study area along National Road QL279, Lao Cai Province, northern Vietnam.

The corridor crosses steep hillslopes, narrow valleys and strongly dissected terrain typical of the northwestern uplands of Vietnam. This road-corridor setting is characterized by short-distance variations in relief, lithology, drainage conditions and human disturbance, making it suitable for examining landslide susceptibility at a corridor scale.

National Road QL279 is an important transport corridor connecting mountainous districts in northern Vietnam. Within Lao Cai Province, it passes through terrain where steep slopes, short drainage lines and heterogeneous slope materials occur over short distances. Landslides along this corridor may interrupt traffic, damage road infrastructure and reduce access to settlements and production areas, particularly during the rainy season. Similar conditions have been reported in other mountainous areas of northern Vietnam, where slope failures are commonly associated with steep topography, concentrated rainfall, weathered materials and human modification of hillslopes (Bui et al., 2011; Kieu and Tran, 2021; Kieu and Ngo, 2022; Do et al., 2025).

The regional relief is shaped by the Hoang Lien Son and Con Voi mountain systems and by the incision of the Red River and its tributaries. Elevation changes rapidly over short distances, producing steep valley sides, high local relief and dense drainage networks. These conditions favour gravitational instability, runoff concentration and toe erosion along valley slopes and road cuts. In the susceptibility model, this terrain setting is represented by DEM-derived variables including elevation, slope, aspect, curvature, stream power index and topographic wetness index, which are widely used to describe topographic and hydrological controls on landslide occurrence (Guzzetti et al., 1999; Van Westen et al., 2008; Reichenbach et al., 2018). These variables are used as spatial conditioning factors and should not be interpreted as deterministic predictors of individual landslide events.

The climate is monsoonal, with rainfall concentrated mainly from late spring to autumn. Seasonal rainfall contributes to slope instability by increasing soil moisture, raising pore-water pressure and reducing the shear resistance of weathered materials. In northern Vietnam, intense and prolonged rainfall has been identified as an important factor in landslides, flash floods and related mountain hazards (Kieu and Tran, 2021; Do et al., 2025; Kieu and Tran, 2025). In this study, rainfall is represented by the maximum 7-day cumulative rainfall derived from CHIRPS data for the 2017–2025 period. Because this rainfall product has a coarser native spatial resolution than the common modelling grid, it is interpreted as a regional hydrometeorological conditioning factor rather than a fine-scale event-triggering variable.

Geologically, the QL279 corridor crosses sedimentary, metasedimentary, metamorphic and intrusive rocks with different weathering characteristics, discontinuity conditions and mechanical resistance. These differences influence the strength of slope-forming materials and their hydrological response during rainfall infiltration. Because lithological changes occur within a narrow road-corridor environment, the area is suitable for testing whether conventional lithological classes can be refined using shear-strength information. This issue is consistent with previous observations that geological variables are more informative in landslide susceptibility modelling when they are parameterized in relation to material behaviour rather than used only as nominal map categories (Bunn et al., 2020; Segoni et al., 2020; Yu et al., 2021). However, the geological information should be interpreted within the limits of its original map scale, even though it is aligned to the common raster grid for GIS overlay and modelling.

Land cover and human disturbance also contribute to spatial variation in slope stability. Vegetation may reduce surface erosion and shallow instability, whereas disturbed surfaces, agricultural land and road-construction zones can modify runoff, infiltration and slope geometry. Road cuts, embankments and drainage modification are particularly relevant in this corridor because they can locally alter slope geometry, runoff pathways and the stability of weathered materials. These factors make the QL279 corridor an appropriate setting for integrating satellite-derived land-cover information with terrain, rainfall, geological and infrastructural variables in a GIS-based susceptibility framework. Overall, the study area provides a representative mountainous road-corridor setting for evaluating the proposed shear-strength-informed lithological standardization approach.

3. DATA AND METHODS

3.1. Research design

This study evaluates whether lithological information can be improved in GIS-based landslide susceptibility modelling by incorporating shear-strength parameters. The workflow included four steps: (1) preparation of the spatial database and landslide inventory; (2) extraction and preprocessing of landslide-conditioning factors; (3) construction of a shear-strength-based Lithological Weakness Index (LWI); and (4) Random Forest modelling, validation and comparison between conventional lithology and LWI-based lithological representation.

All spatial datasets were projected to a common coordinate system, clipped to the study area and aligned to a 12.5 m raster grid defined by the ALOS PALSAR DEM. This grid was used for spatial overlay and modelling consistency. It does not imply that all input datasets have the same original spatial accuracy, especially rainfall data and geological information. Therefore, the 12.5 m grid should be understood as a common computational grid for GIS overlay, sampling and modelling, rather than as an indication of the native spatial resolution, positional accuracy or thematic detail of all predictors.

3.2. Spatial database and conditioning factors

A multi-source spatial database was prepared to represent the main controls on landslide occurrence along the QL279 road corridor. Thirteen conditioning factors were used: elevation, slope, aspect, curvature, stream power index (SPI), topographic wetness index (TWI), normalized difference vegetation index (NDVI), land use/land cover (LULC), maximum 7-day cumulative rainfall, lithology or LWI, distance to roads, distance to rivers and distance to faults. These variables describe terrain morphology, runoff concentration, vegetation condition, land cover, rainfall, geological setting and anthropogenic disturbance, which are widely used in landslide susceptibility studies (Guzzetti et al., 1999; Fell et al., 2008; Van Westen et al., 2008; Reichenbach et al., 2018).

Topographic variables were derived from the ALOS PALSAR DEM. Elevation was used directly, while slope, aspect, curvature, SPI and TWI were calculated from DEM-derived terrain and flow attributes.

Table 1.

Summary of datasets and variables used in the study.

Data source	Product/type	Original resolution/scale	Period	Derived variables
ALOS PALSAR DEM	Digital elevation model	12.5 m	Static	Elevation, slope, aspect, curvature, SPI, TWI
Sentinel-2A	Multispectral imagery	10 m	2017–2025	NDVI
Dynamic World	Land use/land cover product	10 m	2017–2025	LULC
CHIRPS	Gridded precipitation	~5 km	2017–2025	Maximum 7-day cumulative rainfall
Geological/mineral map of Lao Cai Province	Lithological and structural data	1:200,000	Static	Lithology, faults, distance to faults
Road and river networks	Vector line data	Vector	Static/updated where available	Distance to roads, distance to rivers
Google Earth Pro	Historical imagery	Image-dependent	2017–2025	Landslide inventory
Laboratory testing	Shear-strength parameters	58 samples	Field/laboratory campaign	Cohesion, internal friction angle, LWI

NDVI was calculated from Sentinel-2A red and near-infrared bands, and LULC was obtained from the Dynamic World product (Drusch et al., 2012; Brown et al., 2022). Rainfall was represented by the maximum 7-day cumulative rainfall derived from CHIRPS data for 2017–2025.

Because CHIRPS has an original spatial resolution of approximately 5 km, the rainfall raster was resampled only for alignment and was interpreted as a regional hydrometeorological conditioning factor rather than a fine-scale triggering variable (Funk et al., 2015). This treatment avoids assigning unwarranted fine-scale spatial meaning to the resampled rainfall layer.

Geological information was compiled from the geological and mineral map of Lao Cai Province at 1:200,000 scale. The original lithological units were reclassified into seven lithological groups according to lithological similarity, expected mechanical behaviour and the distribution of available shear-strength samples. Fault, road and river vector layers were converted into Euclidean distance rasters. Categorical layers were resampled using the nearest-neighbour method, whereas continuous layers were resampled for alignment with the common modelling grid (**Table 1**). The geological and fault-related variables were therefore used as scale-dependent conditioning factors, and their interpretation remains constrained by the original 1:200,000 map scale.

3.3. Landslide inventory and sample preparation

The landslide inventory was prepared mainly from Google Earth Pro historical imagery for 2017–2025. Landslide scars and disturbed slope surfaces were identified by visual interpretation using morphological and spectral indicators, including bare or recently disturbed surfaces, arcuate or elongated scar forms, downslope accumulation, disrupted vegetation cover and occurrence on steep roadside or valley-side slopes. Multi-temporal imagery was checked where available to reduce confusion between landslide scars and temporary land-cover changes. Such image-based inventories are commonly used in susceptibility modelling where systematic field records are incomplete or spatially inconsistent (Guzzetti et al., 2012; Steger et al., 2017).

Mapped landslide features were converted into landslide-presence samples. In total, 226 landslide samples were used for model training, and 94 samples were reserved for independent testing. A stratified sample split was used so that landslide and non-landslide classes remained balanced in both the training and testing datasets. Accordingly, 226 non-landslide samples were used for training and 94 non-landslide samples were used for independent testing.

Non-landslide samples were selected from areas where no landslides were mapped, excluding water bodies and cells without valid predictor values. To reduce the probability of selecting ambiguous cells close to mapped landslides, a minimum buffer distance of 50 m from the boundary of each mapped landslide polygon was applied before generating non-landslide candidate samples. This distance corresponds to four 12.5 m grid cells and was considered appropriate for reducing boundary uncertainty while retaining sufficient terrain variability within the narrow road-corridor setting. Cells located within mapped landslide polygons or within this 50 m buffer zone were excluded from the non-landslide sampling pool.

The non-landslide sampling was spatially constrained to the same road-corridor modelling extent used for landslide sampling. Candidate non-landslide cells were required to have valid values for all conditioning factors and to fall outside water bodies. No strict matching by slope class or land-cover class was applied, because such matching could artificially reduce the environmental contrast between landslide and non-landslide conditions. However, the candidate pool was kept within the same corridor-scale terrain, lithological and land-cover domain as the landslide samples to ensure that both classes were drawn from comparable spatial conditions. Because absence or pseudo-absence selection can affect susceptibility estimates, the same sampling design was used for both modelling scenarios (Conoscenti et al., 2016; Dou et al., 2020; Gu et al., 2024). This ensured that the comparison between RF-Lithology and RF-LWI reflected the effect of lithological representation rather than differences in sampling strategy.

3.4. Shear-strength-based lithological standardization

The main methodological contribution of this study is the conversion of lithology from a nominal categorical predictor into a shear-strength-informed variable. Laboratory-derived cohesion and internal friction angle from 58 samples were used to characterize the seven reclassified lithological groups. These parameters were selected because they are directly related to shear resistance and are commonly used to describe the mechanical behaviour of slope-forming materials. The number of samples per lithological group ranged from 7 to 9, providing a first-order basis for estimating group-level shear-strength conditions. However, these samples should be interpreted as representative of average lithological-group behaviour rather than as a complete description of local variability in weathering grade, discontinuity density, groundwater condition or rock-mass structure.

Cohesion and internal friction angle were first normalized using min–max normalization:

$$c_{norm} = \frac{c - c_{min}}{c_{max} - c_{min}} \tag{1}$$

$$\phi_{norm} = \frac{\phi - \phi_{min}}{\phi_{max} - \phi_{min}} \tag{2}$$

where c_{norm} and ϕ_{norm} are the normalized cohesion and internal friction angle; $c$and $\phi$are the measured cohesion and internal friction angle; and the subscripts min and max denote the minimum and maximum values in the sample dataset.

A composite Shear Strength Index (SSI) was calculated as:

$$SSI = 0.5c_{norm} + 0.5\phi_{norm} \tag{3}$$

Equal weights were used as a neutral and transparent assumption because cohesion and internal friction angle represent complementary components of shear strength. Cohesion reflects the bonding or cementation component of material resistance, whereas the internal friction angle reflects frictional resistance along potential failure surfaces. In the absence of an independent calibration dataset or prior evidence supporting unequal contributions of these two parameters for all lithological groups, assigning different weights would introduce additional subjectivity.

The Lithological Weakness Index was then defined as:

$$LWI = 1 - SSI \tag{4}$$

The LWI ranges from 0 to 1. Higher values indicate weaker lithological conditions, whereas lower values indicate stronger mechanical conditions. Mean LWI values were assigned to the corresponding lithological groups and rasterized to the 12.5 m grid. This procedure represents lithology as a mechanical weakness gradient rather than only as a nominal geological class, following recent recommendations that geological and rock–soil information should be parameterized in relation to material behaviour when used in susceptibility modelling (Bunn et al., 2020; Segoni et al., 2020; Yu et al., 2021). The LWI is therefore used as a standardized lithological weakness proxy for susceptibility modelling, not as a substitute for detailed site-specific geotechnical investigation.

3.5. Random Forest modelling

Landslide susceptibility was modelled using Random Forest, an ensemble-learning algorithm that builds multiple decision trees from bootstrap samples and random subsets of predictors (Breiman, 2001). Random Forest was selected because it can model nonlinear relationships, handle mixed predictor types and provide variable-importance measures. It has been widely used in landslide susceptibility studies and has shown stable performance in complex terrain (Catani et al., 2013; Chen et al., 2018; Merghadi et al., 2020; Ado et al., 2022).

The model was configured with 300 trees. At each split, the number of candidate predictors was determined using the square-root rule. A balanced subsampling strategy was applied to reduce the effect of class imbalance. Two model scenarios were developed using the same training and testing samples and the same Random Forest configuration: (1) RF-Lithology, in which lithology was represented by the seven reclassified lithological groups; (2) RF-LWI, in which the lithological predictor was replaced by the shear-strength-derived LWI. Using identical samples, predictors other than lithology, and model settings allowed the effect of lithological representation to be isolated as much as possible.

The RF-LWI model produced a continuous landslide susceptibility probability. For map production, this output was classified into five susceptibility levels: very low, low, moderate, high and very high, using the natural breaks method. The same classification procedure was used consistently for susceptibility mapping and area statistics. The resulting classes represent relative susceptibility levels within the study area and should not be interpreted as deterministic hazard classes or as estimates of landslide timing or magnitude.

3.6. Model validation and comparison

Model performance was evaluated using the independent testing dataset and repeated stratified cross-validation. The confusion matrix was used to derive accuracy, precision, recall and F1-score. The area under the receiver operating characteristic curve (AUC-ROC) was used as a threshold-independent measure of discrimination between landslide and non-landslide samples (Chung and Fabbri, 2003; Fawcett, 2006; Reichenbach et al., 2018).

To assess model stability, repeated stratified 5-fold cross-validation with 10 repetitions was applied. Mean values, standard deviations and 95% confidence intervals were calculated for AUC-ROC, accuracy, precision, recall, F1-score and out-of-bag score. The 95% confidence interval of AUC on the independent testing dataset was estimated by bootstrap resampling with 1,000 iterations.

The RF-Lithology and RF-LWI scenarios were compared using the same validation procedure. Paired t-tests and Wilcoxon signed-rank tests were applied to the repeated validation results to evaluate whether the difference between the two lithological representations was statistically meaningful. These paired tests were based on 50 paired validation results obtained from the repeated stratified 5-fold cross-validation procedure, calculated as 5 folds × 10 repetitions. Each pair compared RF-Lithology and RF-LWI under the same fold and repetition, thereby reducing the influence of random data partitioning on the model comparison.

Variable importance was examined using Gini importance and permutation importance. Gini importance measures the average decrease in node impurity, whereas permutation importance measures the decrease in model performance after randomly permuting each predictor. Using both measures supports a more cautious interpretation of predictor contribution, particularly where conditioning factors may be spatially correlated.

Finally, the classified RF-LWI susceptibility map was evaluated by overlaying landslide samples on susceptibility classes and by constructing success-rate and prediction-rate curves. Area statistics were calculated for each susceptibility class to quantify the spatial distribution of landslide-prone terrain along the road corridor. The overlay and rate-curve analyses were used as complementary spatial validation procedures, while the independent testing dataset and repeated cross-validation remained the primary basis for quantitative model assessment.

4. RESULTS

4.1. Lithological weakness derived from shear-strength standardization

The shear-strength-based standardization revealed clear differences in relative mechanical weakness among the seven reclassified lithological groups. The mean Lithological Weakness Index (LWI) ranged from 0.406 to 0.858, indicating that the lithological groups are not equivalent in terms of shear-strength-related behaviour. The highest mean LWI was obtained for the coarse clastic/red-

bed sequence, whereas the lowest value was observed for the carbonate-bearing metasedimentary sequence. Intermediate LWI values were found in the fine clastic/coal-bearing sedimentary sequence, metasedimentary schist–quartzite sequence, high-grade metamorphic gneiss–amphibolite sequence, felsic intrusive–subvolcanic association and mafic to ultramafic intrusive association.

The high LWI value of the coarse clastic/red-bed sequence mainly reflects its lower mean cohesion relative to the other groups. In contrast, the carbonate-bearing metasedimentary sequence shows the lowest LWI, indicating comparatively stronger lithological conditions within the standardized dataset. Because each lithological group was represented by 7–9 shear-strength samples, these values should be interpreted as group-level indicators of relative lithological weakness rather than complete geotechnical descriptions of local rock-mass conditions. The results are summarized in **Table 2.**

Table 2.

Shear-strength-based Lithological Weakness Index values of reclassified lithological groups.

Lithological group	Reclassified lithological group	n	Mean cohesion (kPa)	Mean friction angle (°)	Mean LWI	LWI range
1	Carbonate-bearing metasedimentary sequence	8	26.128	31.240	0.406	0.362–0.456
2	Fine clastic / coal-bearing sedimentary sequence	8	30.129	30.598	0.483	0.285–0.620
3	Coarse clastic / red-bed sequence	9	15.816	30.487	0.858	0.742–0.949
4	Medium-grade metasedimentary schist–quartzite sequence	8	26.101	30.889	0.501	0.320–0.858
5	High-grade metamorphic gneiss–amphibolite sequence	9	29.128	30.596	0.507	0.326–0.798
6	Felsic intrusive–subvolcanic association	7	25.304	30.389	0.655	0.547–0.786
7	Mafic to ultramafic intrusive association	9	26.729	30.458	0.602	0.489–0.767

4.2. Predictive performance of the RF-LWI model

The RF-LWI model produced satisfactory predictive performance on the independent testing dataset. The confusion matrix included 94 true negatives, 4 false positives, 22 false negatives and 72 true positives. The model achieved an AUC-ROC of 0.936, with a 95% confidence interval of 0.900–0.966. Accuracy, precision, recall and F1-score were 0.865, 0.947, 0.766 and 0.847, respectively, and the OOB score was 0.879 (**Table 3**). These results indicate good discrimination and high precision, although the recall value shows that some landslide samples were not detected at the selected classification threshold.

Table 3.

Confusion matrix and performance metrics of the RF-LWI model.

Model	TN	FP	FN	TP	AUC-ROC	AUC 95% CI	Accuracy	Precision	Recall	F1-score	OOB score
RF-LWI	94	4	22	72	0.936	0.900–0.966	0.865	0.947	0.766	0.847	0.879

The validation results are shown graphically in **Fig. 2**. The ROC curve confirms good discrimination between landslide and non-landslide samples. The confusion matrix also indicates that the model produced few false positives, although a number of landslide samples were not detected at the selected threshold.

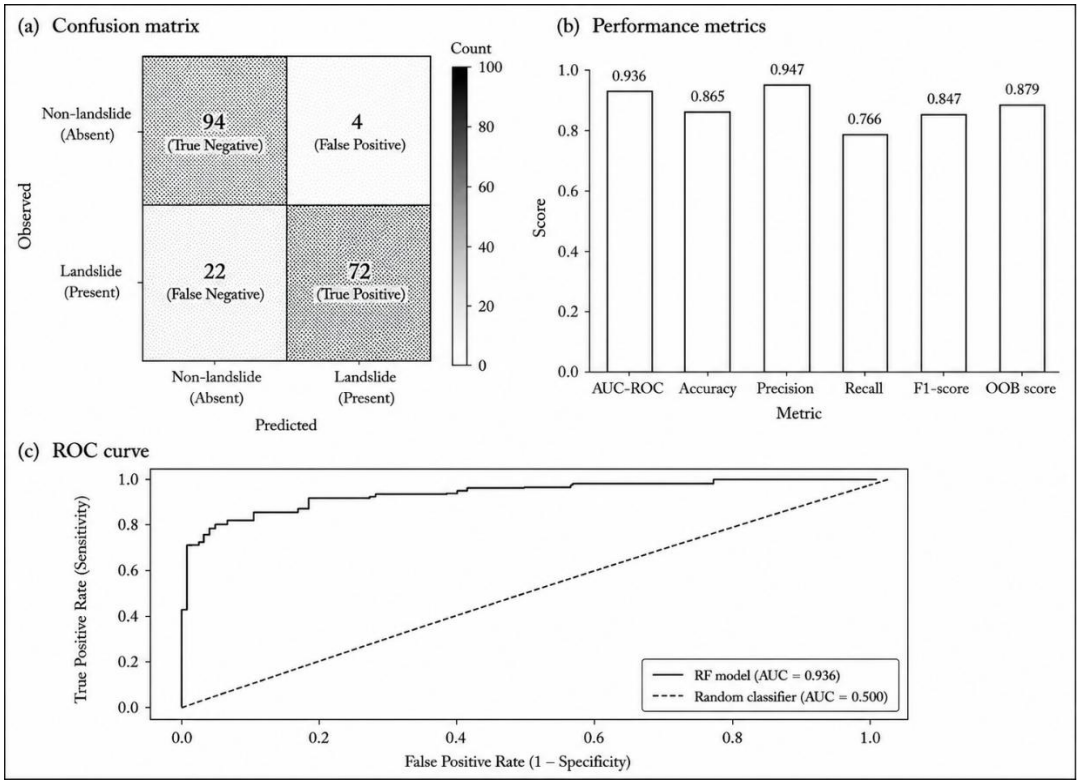

Fig. 2. Validation results of the RF-LWI model, including (a) confusion matrix, (b) performance metrics and (c) ROC curve.

Repeated stratified 5-fold cross-validation with 10 repetitions confirmed the stability of the RF-LWI model. The mean cross-validated AUC-ROC was 0.943, with a standard deviation of 0.020 and a 95% confidence interval of 0.901–0.974. Mean accuracy, precision, recall and F1-score were 0.884, 0.942, 0.823 and 0.877, respectively, while the mean OOB score was 0.883 (**Table 4**).

Table 4.
Repeated stratified 5-fold cross-validation results of the RF-LWI model.

Metric	Mean	SD	95% CI
AUC-ROC	0.943	0.020	0.901–0.974
Accuracy	0.884	0.030	0.821–0.942
Precision	0.942	0.037	0.875–1.000
Recall	0.823	0.049	0.739–0.911
F1-score	0.877	0.032	0.812–0.939
OOB score	0.883	0.008	0.869–0.896

Note: The cross-validation results were obtained from 50 validation runs, calculated as 5 folds × 10 repetitions.

4.3. Effect of shear-strength-based lithological standardization

The RF-LWI and RF-Lithology models were compared to evaluate the effect of replacing conventional reclassified lithology with the shear-strength-derived LWI. On the independent testing dataset, the RF-LWI model showed slightly higher values for most performance metrics. AUC-ROC increased from 0.935 to 0.936, accuracy from 0.849 to 0.865, precision from 0.933 to 0.947, recall

from 0.745 to 0.766 and F1-score from 0.828 to 0.847. The number of false positives decreased from 5 to 4, and false negatives decreased from 24 to 22 (**Table 5**). These differences indicate a modest improvement rather than a substantial change in predictive performance.

Table 5.

Comparison of Random Forest model performance using reclassified lithology and shear-strength-derived Lithological Weakness Index.

Model	Lithological variable	TN	FP	FN	TP	AUC-ROC	Accuracy	Precision	Recall	F1-score
RF-Lithology	Reclassified lithology	93	5	24	70	0.935	0.849	0.933	0.745	0.828
RF-LWI	Shear-strength-derived LWI	94	4	22	72	0.936	0.865	0.947	0.766	0.847

The repeated validation results were also compared statistically. The AUC-ROC difference between RF-LWI and RF-Lithology was significant according to both the paired t-test and the Wilcoxon signed-rank test. In contrast, the F1-score difference was not statistically significant. These results indicate that the LWI-based representation improved model discrimination, while the overall classification improvement remained limited. The statistical comparison is presented in **Table 6**.

Table 6.

Statistical comparison between RF-Lithology and RF-LWI models based on repeated validation results.

Metric	Statistical test	Difference RF-LWI − RF-Lithology	p-value	Result
AUC-ROC	Paired t-test	0.0065	0.043	Significant
AUC-ROC	Wilcoxon signed-rank test	0.0065	0.035	Significant
F1-score	Paired t-test	−0.0022	0.322	Not significant
F1-score	Wilcoxon signed-rank test	−0.0022	0.317	Not significant

Note: The paired tests were based on 50 paired validation results obtained from repeated stratified 5-fold cross-validation with 10 repetitions.

4.4. Landslide susceptibility pattern

The RF-LWI model was used to generate the final landslide susceptibility map. The predicted susceptibility values were classified into five levels: very low, low, moderate, high and very high. The map shows that high and very high susceptibility classes are mainly distributed along steep valley-side slopes, road-adjacent sectors and areas where weak lithological conditions coincide with drainage concentration (**Fig. 3**).

The area statistics indicate that the very high susceptibility class occupies 215.180 km², corresponding to 35.08% of the study area. The high susceptibility class covers 108.108 km², or 17.63%. Together, the high and very high susceptibility classes account for 52.71% of the study area. The moderate, low and very low classes account for 14.84%, 26.72% and 5.73%, respectively. These statistics are presented in **Table 7**.

Table 7.
Area statistics of landslide susceptibility classes.

Class	Susceptibility level	Pixel count	Area (km²)	Area (%)
1	Very low	224,779	35.122	5.73
2	Low	1,049,006	163.907	26.72
3	Moderate	582,557	91.025	14.84
4	High	691,890	108.108	17.63
5	Very high	1,377,149	215.180	35.08

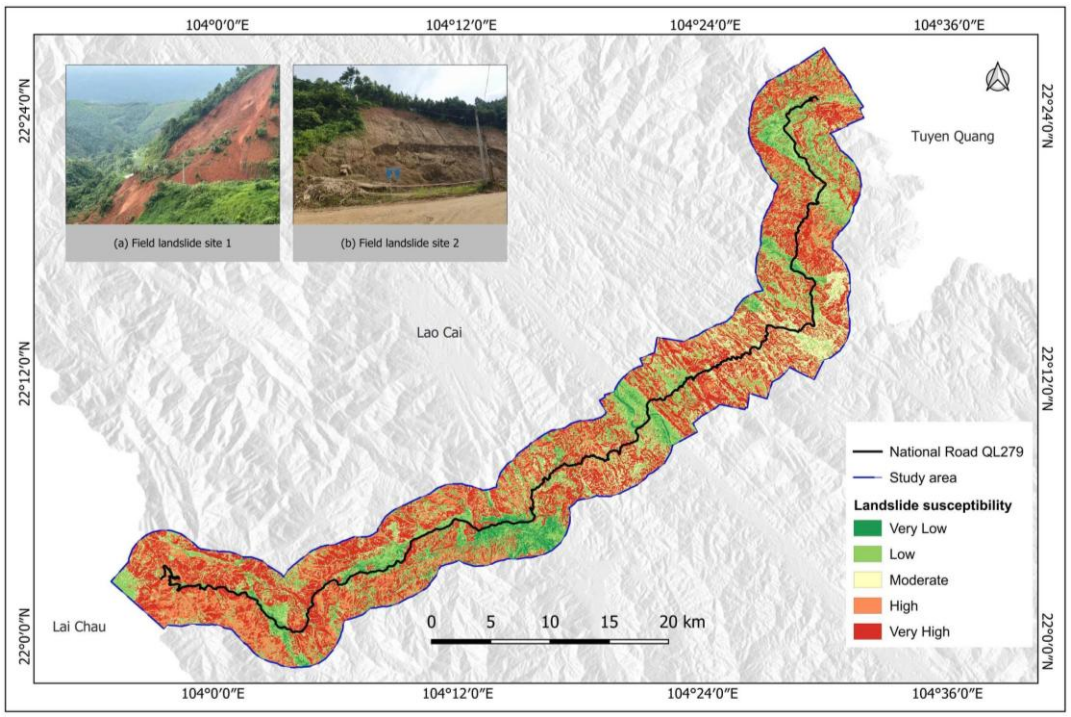

Fig. 3. Landslide susceptibility map generated by the RF-LWI model.

4.5. Spatial validation and variable importance

The spatial validation was conducted by overlaying the training and testing landslide samples on the RF-LWI susceptibility map. Most landslide samples are located within the high and very high susceptibility classes, indicating spatial consistency between the model output and the observed landslide distribution (**Fig. 4**).

The success-rate and prediction-rate curves provide additional information on the distribution of landslide samples across susceptibility values. The curves show that landslide samples are concentrated within the upper susceptibility ranges. The success-rate curve reflects the fit to the training samples, whereas the prediction-rate curve reflects model performance on the independent testing samples (**Fig. 5**).

Variable-importance analysis indicates that slope was the most influential predictor in the RF-LWI model. Other relevant variables included distance to roads, rainfall, LWI, distance to rivers and selected terrain indices. The Gini and permutation importance measures produced broadly consistent patterns, although the relative ranking of some variables differed (**Fig. 6**).

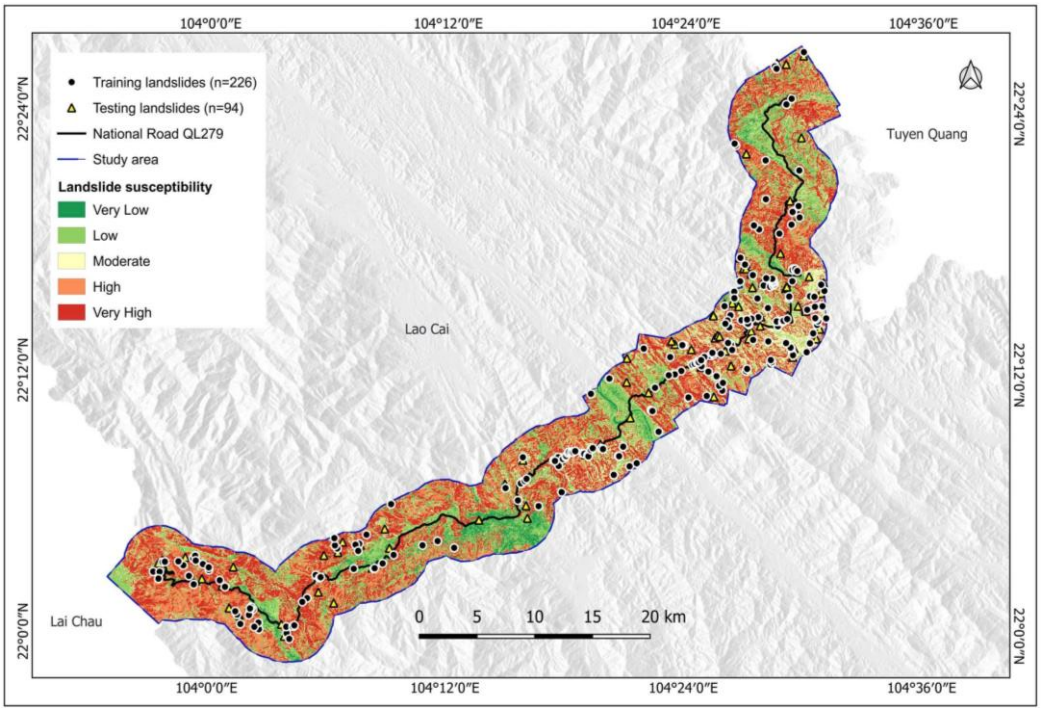

Fig. 4. Spatial validation of the landslide susceptibility map using observed landslide inventory points. Training and testing samples are overlaid on the susceptibility map.

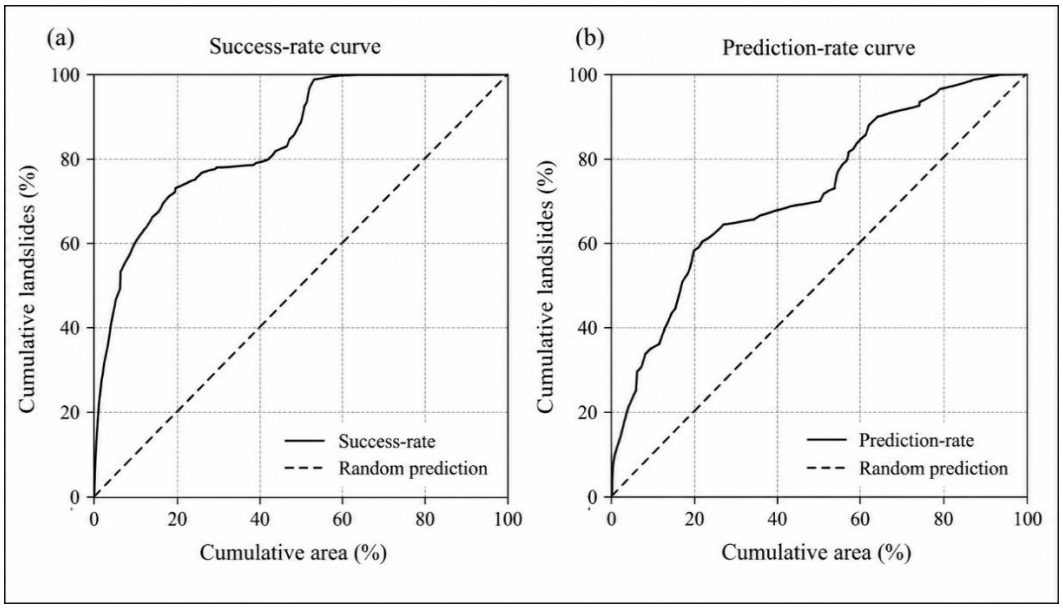

Fig. 5. Success-rate and prediction-rate curves of the landslide susceptibility model: (a) success-rate curve derived from training landslide samples and (b) prediction-rate curve derived from independent testing samples.

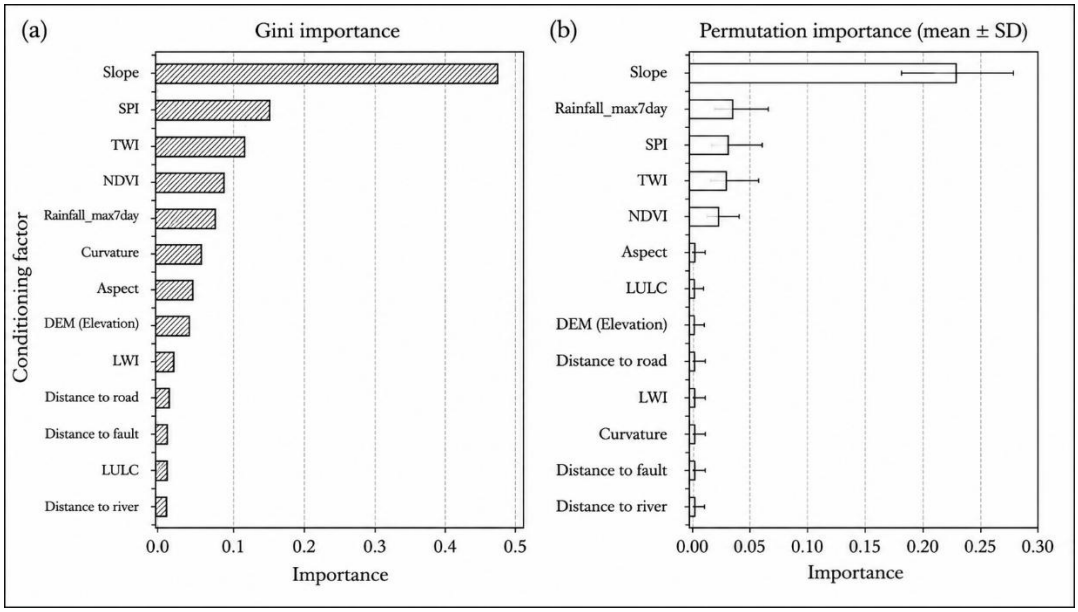

Fig. 6. Variable importance of conditioning factors: (a) Gini importance derived from the Random Forest model and (b) permutation importance.

Overall, the results show that the RF-LWI model produced stable predictive performance and a spatially coherent susceptibility pattern. The shear-strength-derived LWI provided a small but statistically detectable improvement in discrimination and improved the interpretability of the lithological predictor, while the overall classification improvement remained limited.

5. DISCUSSION

The results indicate that shear-strength-informed lithological standardization provides a useful refinement for representing lithology in GIS-based landslide susceptibility modelling. By deriving a Lithological Weakness Index (LWI) from cohesion and internal friction angle, lithology was expressed as a continuous mechanical weakness gradient rather than only as a nominal geological class. This approach is relevant because mapped lithological units do not always reflect the mechanical behaviour of weathered slope-forming materials, particularly in structurally complex mountainous terrain. The result is consistent with previous studies emphasizing that geological and rock–soil information should be parameterized in relation to material properties when used in susceptibility modelling (Bunn et al., 2020; Segoni et al., 2020; Yu et al., 2021). However, the LWI should be interpreted as a group-level proxy for relative lithological weakness, not as a complete geotechnical characterization of each geological unit.

The RF-LWI model produced satisfactory predictive performance, with an independent-test AUC-ROC of 0.936 and a mean cross-validated AUC-ROC of 0.943. These values are comparable with previous GIS- and machine-learning-based landslide susceptibility studies, in which Random Forest has been shown to perform well in complex terrain because of its capacity to model nonlinear relationships among conditioning factors (Catani et al., 2013; Chen et al., 2018; Merghadi et al., 2020; Ado et al., 2022).

The high precision and lower recall indicate that the model produced relatively few false positive classifications, but still missed part of the observed landslide class. This trade-off is relevant for road-corridor applications because field inspection and maintenance planning should consider not only very high susceptibility sectors, but also areas where landslides may be under-detected at the selected classification threshold.

The comparison between RF-Lithology and RF-LWI shows that the use of LWI produced a modest improvement. The increase in AUC-ROC was statistically significant in repeated validation, whereas the difference in F1-score was not significant. Therefore, the main contribution of LWI should be interpreted as improving model discrimination and geological interpretability rather than producing a large increase in overall classification accuracy. This interpretation is consistent with the paired validation design, in which the two models were compared using the same samples, predictors other than lithology and Random Forest settings. It also reflects the multi-factor nature of landslide occurrence along mountainous road corridors, where slope, rainfall, drainage, road-related disturbance and lithological weakness interact rather than act independently.

The spatial pattern of susceptibility is consistent with the geomorphological setting of the QL279 corridor. High and very high susceptibility classes are concentrated mainly along steep valley-side slopes, road-adjacent sectors and areas where weak lithological conditions coincide with drainage concentration. Similar controls have been reported in northern Vietnam and other mountainous environments, where slope gradient, rainfall, weathered materials and human modification of hillslopes are important contributors to slope instability (Bui et al., 2011; Kieu and Tran, 2021; Kieu and Ngo, 2022; Do et al., 2025). The overlay of landslide samples on the susceptibility map and the success-rate and prediction-rate curves further support the spatial consistency of the model output. Because the susceptibility classes were derived from modelled probability values using the natural breaks method, they should be interpreted as relative susceptibility levels within the study area rather than deterministic hazard or risk classes, which would require explicit information on landslide timing, magnitude and exposure (Fell et al., 2008; Van Westen et al., 2008; Reichenbach et al., 2018).

Variable-importance results confirm the dominant role of slope in the RF-LWI model, which is reasonable because slope controls the gravitational component acting on hillslope materials and influences runoff and erosion processes. Distance to roads, rainfall, LWI, distance to rivers and terrain indices also contributed to prediction. The role of distance to roads reflects the influence of slope cutting, embankments and drainage modification in road-corridor environments, while rainfall and distance to rivers represent hydrological controls. The contribution of LWI indicates that lithological weakness is relevant, but it does not dominate the model. Thus, shear-strength-based lithological standardization should be considered a refinement of the geological component rather than a replacement for topographic, hydrological and infrastructural predictors.

Several limitations should be acknowledged. The landslide inventory was compiled mainly from Google Earth Pro historical imagery; therefore, small, old or vegetation-covered landslides may have been omitted, which can affect model training and validation (Guzzetti et al., 2012; Steger et al., 2017). The selection of non-landslide samples is another source of uncertainty because different absence-sampling strategies can influence model performance and prediction patterns (Conoscenti et al., 2016; Dou et al., 2020; Gu et al., 2024). Although this study applied a 50 m exclusion buffer around mapped landslide polygons and used the same balanced sampling design for both model scenarios, pseudo-absence selection cannot completely eliminate uncertainty in areas where unmapped, old or dormant landslides may exist. In addition, the 58 shear-strength samples provide a first-order basis for calculating LWI across the seven lithological groups, but they cannot fully represent local variations in weathering grade, discontinuity density, groundwater conditions or rock-mass structure. Similarly, the use of a common 12.5 m raster grid improves spatial overlay and modelling consistency, but it does not remove the original scale limitations of the CHIRPS rainfall data or the 1:200,000 geological map. These scale constraints should be considered when interpreting fine-scale susceptibility patterns.

Future work should test the LWI approach in other mountainous road corridors and geological settings. Additional engineering-geological data, including weathering grade, discontinuity characteristics, groundwater conditions and rock-mass quality, would help refine the lithological weakness representation. Further research should also examine alternative weighting schemes for cohesion and internal friction angle, compare the approach with other machine-learning algorithms, and integrate temporal rainfall information and road-exposure data to support more operational landslide-risk assessment.

6. CONCLUSIONS

This study proposed a shear-strength-informed lithological standardization approach for GIS-based landslide susceptibility modelling along a mountainous road corridor in northern Vietnam. Reclassified lithological groups were converted into a Lithological Weakness Index (LWI) using laboratory-measured cohesion and internal friction angle and integrated into a Random Forest model. The RF-LWI model showed stable predictive performance, with an independent-test AUC-ROC of 0.936 and a mean cross-validated AUC-ROC of 0.943; high and very high susceptibility classes covered 52.71% of the study area, mainly along steep valley-side slopes, road-adjacent sectors and areas where weak lithological conditions coincide with drainage concentration. Compared with conventional lithological representation, the LWI-based model produced a modest improvement in discrimination, while threshold-dependent classification improvement remained limited. The main contribution of the approach is therefore the improved physical interpretability of the lithological predictor rather than a large increase in predictive accuracy. The resulting map can support preliminary identification of road sections requiring field inspection, drainage maintenance or slope-stabilization assessment, but the susceptibility classes should be interpreted as relative levels within the study area rather than deterministic hazard or risk classes. Future work should test the transferability of the LWI approach in other geological settings and incorporate additional engineering-geological information, including weathering grade, discontinuity characteristics, groundwater conditions and rock-mass quality.

ACKNOWLEDGEMENTS

This research was supported by Thai Nguyen University, Vietnam, under Grant No. ĐH2026-TN01-12. The authors gratefully acknowledge this support and the data provided for this study.

REFERENCES

Ado, M., Khwairakpam, A., Maji, A.K., Jasińska, E., Gono, R., Leonowicz, Z. and Jasiński, M. (2022) Landslide susceptibility mapping using machine learning: a literature survey. Remote Sensing, 14(13), 3029. DOI: 10.3390/rs14133029.

Breiman, L. (2001) Random forests. Machine Learning, 45(1), 5–32. DOI: 10.1023/A:1010933404324.

Brown, C.F., Brumby, S.P., Guzder-Williams, B. et al. (2022) Dynamic World, near real-time global 10 m land use land cover mapping. Scientific Data, 9, 251. DOI: 10.1038/s41597-022-01307-4.

Bui, D.T., Lofman, O., Revhaug, I. and Dick, O. (2011) Landslide susceptibility analysis in the Hoa Binh province of Vietnam using statistical index and logistic regression. Natural Hazards, 59(3), 1413–1444. DOI: 10.1007/s11069-011-9844-2.

Bunn, M., Leshchinsky, B. and Olsen, M.J. (2020) Geologic trends in shear strength properties inferred through three-dimensional back analysis of landslide inventories. Journal of Geophysical Research: Earth Surface, 125(9), e2019JF005461. DOI: 10.1029/2019JF005461.

Catani, F., Lagomarsino, D., Segoni, S. and Tofani, V. (2013) Landslide susceptibility estimation by random forests technique: sensitivity and scaling issues. Natural Hazards and Earth System Sciences, 13(11), 2815–2831. DOI: 10.5194/nhess-13-2815-2013.

Chen, W., Xie, X., Peng, J., Shahabi, H., Hong, H., Bui, D.T., Duan, Z. and Zhu, A.X. (2018) GIS-based landslide susceptibility evaluation using a novel hybrid integration approach of bivariate statistical based random forest method. Catena, 164, 135–149. DOI: 10.1016/j.catena.2018.01.012.

Chung, C.J.F. and Fabbri, A.G. (2003) Validation of spatial prediction models for landslide hazard mapping. Natural Hazards, 30(3), 451–472. DOI: 10.1023/B.0000007172.62651.2B.

Conoscenti, C., Rotigliano, E., Cama, M., Caraballo-Arias, N.A., Lombardo, L. and Agnesi, V. (2016) Exploring the effect of absence selection on landslide susceptibility models: a case study in Sicily, Italy. Geomorphology, 261, 222–235. DOI: 10.1016/j.geomorph.2016.03.006.

Dahmani, L., Laaribya, S., Naim, H. and Dindaroglu, T. (2025) Development and assessment of landslide susceptibility in the province of Chefchaouen, North-West Morocco, using remote sensing and GIS: a weighted overlay analysis approach. Geographia Technica, 20(2), 1–14. DOI: 10.21163/GT_2025.202.01.

Do, T.V.H., Pham, H.G., Kieu, Q.L. and Tran, T.N.H. (2025) The typical mechanisms and factors leading to flash floods in small watersheds in the mountainous region of Vietnam: a case study in the Chu Va stream watershed. Larhyss Journal, 61, 141–168. Available at:

https://www.larhyss.net/ojs/index.php/larhyss/article/view/16732.

Dou, J., Yunus, A.P., Merghadi, A., Shirzadi, A., Nguyen, H., Hussain, Y., Avtar, R., Chen, Y., Pham, B.T. and Yamagishi, H. (2020) Different sampling strategies for predicting landslide susceptibilities are deemed less consequential with deep learning. Science of the Total Environment, 720, 137320. DOI: 10.1016/j.scitotenv.2020.137320.

Drusch, M., Del Bello, U., Carlier, S., Colin, O., Fernandez, V., Gascon, F., Hoersch, B., Isola, C., Laberinti, P., Martimort, P. et al. (2012) Sentinel-2: ESA's optical high-resolution mission for GMES operational services. Remote Sensing of Environment, 120, 25–36. DOI: 10.1016/j.rse.2011.11.026.

Edial, H., Iskarni, P., Purwaningsih, E., Wilis, R., Chandra, D., Hafnil, J. and Desman, S. (2025) GIS-based landslide vulnerability mapping along the Sumatran Fault: a case study in Pasaman Regency, Indonesia. Geographia Technica, 20(1), 228–248. DOI: 10.21163/GT_2025.201.16.

Fawcett, T. (2006) An introduction to ROC analysis. Pattern Recognition Letters, 27(8), 861–874. DOI: 10.1016/j.patrec.2005.10.010.

Fell, R., Corominas, J., Bonnard, C., Cascini, L., Leroi, E. and Savage, W.Z. (2008) Guidelines for landslide susceptibility, hazard and risk zoning for land use planning. Engineering Geology, 102(3–4), 85–98. DOI: 10.1016/j.enggeo.2008.03.022.

Funk, C., Peterson, P., Landsfeld, M., Pedreros, D., Verdin, J., Shukla, S., Husak, G., Rowland, J., Harrison, L., Hoell, A. and Michaelsen, J. (2015) The climate hazards infrared precipitation with stations — a new environmental record for monitoring extremes. Scientific Data, 2, 150066. DOI: 10.1038/sdata.2015.66.

Gu, T., Li, J., Wang, M., Duan, P., Zhang, Y. and Cheng, L. (2023) Study on landslide susceptibility mapping with different factor screening methods and random forest models. PLOS ONE, 18(10), e0292897. DOI: 10.1371/journal.pone.0292897.

Gu, T., Duan, P., Wang, M., Li, J. and Zhang, Y. (2024) Effects of non-landslide sampling strategies on machine learning models in landslide susceptibility mapping. Scientific Reports, 14, 7201. DOI: 10.1038/s41598-024-57964-5.

Guzzetti, F., Carrara, A., Cardinali, M. and Reichenbach, P. (1999) Landslide hazard evaluation: a review of current techniques and their application in a multi-scale study, central Italy. Geomorphology, 31(1–4), 181–216. DOI: 10.1016/S0169-555X(99)00078-1.

Guzzetti, F., Mondini, A.C., Cardinali, M., Fiorucci, F., Santangelo, M. and Chang, K.-T. (2012) Landslide inventory maps: new tools for an old problem. Earth-Science Reviews, 112(1–2), 42–66. DOI: 10.1016/j.earscirev.2012.02.001.

Kanwar, M., Pokharel, B. and Lim, S. (2025) A new random forest method for landslide susceptibility mapping using hyperparameter optimization and grid search techniques. International Journal of Environmental Science and Technology, 22, 10635–10650. DOI: 10.1007/s13762-024-06310-3.

Kieu, Q.L. and Ngo, G.V. (2022) Landslide susceptibility assessment for warning of dangerous areas in Tan Uyen district, Lai Chau province, Vietnam. Geografiska Annaler: Series A, Physical Geography, 104(3), 183–200. DOI: 10.1080/04353676.2022.2091915.

Kieu, Q.L. and Tran, D.V. (2021) Application of geospatial technologies in constructing a flash flood warning model in northern mountainous regions of Vietnam: a case study at Trinh Tuong commune, Bat Xat district, Lao Cai province. Bulletin of Geography. Physical Geography Series, 20, 31–43. DOI: 10.2478/bgeo-2021-0003.

Kieu, Q.L. and Tran, T.N.H. (2025) Assessing livelihood vulnerability to climate change and disasters in northern Vietnam. Theoretical and Applied Climatology, 156, 610. DOI: 10.1007/s00704-025-05842-z.

Merghadi, A., Yunus, A.P., Dou, J., Whiteley, J., Thai Pham, B., Bui, D.T., Avtar, R. and Shirzadi, A. (2020) Machine learning methods for landslide susceptibility studies: a comparative overview of algorithm performance. Earth-Science Reviews, 207, 103225. DOI: 10.1016/j.earscirev.2020.103225.

Reichenbach, P., Rossi, M., Malamud, B.D., Mihir, M. and Guzzetti, F. (2018) A review of statistically-based landslide susceptibility models. Earth-Science Reviews, 180, 60–91. DOI: 10.1016/j.earscirev.2018.03.001.

Segoni, S., Pappafico, G., Luti, T. and Catani, F. (2020) Landslide susceptibility assessment in complex geological settings: sensitivity to geological information and insights on its parameterization. Landslides, 17(10), 2443–2453. DOI: 10.1007/s10346-019-01340-2.

Steger, S., Brenning, A., Bell, R. and Glade, T. (2017) The influence of systematically incomplete shallow landslide inventories on statistical susceptibility models and suggestions for improvements. Landslides, 14(5), 1767–1781. DOI: 10.1007/s10346-017-0820-0.

Tanyu, B.F., Abbaspour, A., Alimohammadlou, Y. and Tecuci, G. (2021) Landslide susceptibility analyses using Random Forest, C4.5, and C5.0 with balanced and unbalanced datasets. Catena, 203, 105355. DOI: 10.1016/j.catena.2021.105355.

Van Westen, C.J., Castellanos, E. and Kuriakose, S.L. (2008) Spatial data for landslide susceptibility, hazard, and vulnerability assessment: an overview. Engineering Geology, 102(3–4), 112–131. DOI: 10.1016/j.enggeo.2008.03.010.

Yu, X., Zhang, K., Song, Y., Jiang, W. and Zhou, J. (2021) Study on landslide susceptibility mapping based on rock-soil characteristic factors. Scientific Reports, 11, 15476. DOI: 10.1038/s41598-021-94936-5.

Zhanabayev, D., Dzhanaleeva, K., Atasoy, E. and Efe, R. (2024) Landslide susceptibility mapping using Analytical Hierarchy Process and Geographical Information System in Rudny Altai Region, East Kazakhstan. Geographia Technica, 19(1), 151–165. DOI: 10.21163/GT_2024.191.11.